

32. Saito, R. Physical properties of carbon nanotubes [Text] / R. Saito, G. Dresselhaus, M. S. Dresselhaus. – London: Imperial College Press, 1998. – 272 p.
33. Imry, Y. Conductance viewed as transmission [Text] / Y. Imry, R. Landauer // Reviews of Modern Physics. – 1999. – Vol. 71, Issue 2. – P. S306–S312. doi: 10.1103/revmodphys.71.s306
34. Buldum, A. Contact resistance between carbon nanotubes [Text] / A. Buldum, J. P. Lu // Physical Review B. – 2001. – Vol. 63, Issue 16. doi: 10.1103/physrevb.63.161403
35. Naeemi, A. Performance Modeling for Carbon Nanotube Interconnects [Text] / A. Naeemi, J. D. Meindl // Integrated Circuits and Systems. – 2008. – P. 163–190. doi: 10.1007/978-0-387-69285-2_7
36. Hertel, T. Deformation of carbon nanotubes by surface van der Waals forces [Text] / T. Hertel, R. E. Walkup, P. Avouris // Physical Review B. – 1998. – Vol. 58, Issue 20. – P. 13870–13873. doi: 10.1103/physrevb.58.13870
37. Girifalco, L. A. Carbon nanotubes, buckyballs, ropes, and a universal graphitic potential [Text] / L. A. Girifalco, M. Hodak, R. S. Lee // Physical Review B. – 2000. – Vol. 62, Issue 19. – P. 13104–13110. doi: 10.1103/physrevb.62.13104
38. Simmons, J. G. Generalized Formula for the Electric Tunnel Effect between Similar Electrodes Separated by a Thin Insulating Film [Text] / J. G. Simmons // Journal of Applied Physics. – 1963. – Vol. 34, Issue 6. – P. 1793–1804. doi: 10.1063/1.1702682
39. Li, X. S. An overview of SuperLU [Text] / X. S. Li // ACM Transactions on Mathematical Software. – 2005. – Vol. 31, Issue 3. – P. 302–325. doi: 10.1145/1089014.1089017
40. Demmel, J. W. SuperLU users guide [Text] / J. W. Demmel, J. R. Gilbert, X. S. Li. – Lawrence Berkeley National Laboratory, 1999. doi: 10.2172/751785
41. Demmel, J. W. A Supernodal Approach to Sparse Partial Pivoting [Text] / J. W. Demmel, S. C. Eisenstat, J. R. Gilbert, X. S. Li, J. W. H. Liu // SIAM Journal on Matrix Analysis and Applications. – 1999. – Vol. 20, Issue 3. – P. 720–755. doi: 10.1137/s0895479895291765

Запропоновано методику визначення параметрів виділення кисню на оксиднонікеловому електроді. Пропонована методика застосована для вивчення процесу виділення кисню на зразках гідроксиду нікелю, отриманих різними способами і для різних фракцій. Визначено ефективні константи рівняння Тафеля. Показано, що параметри виділення кисню залежать від методу отримання гідроксиду нікелю (II) та його фракційного складу

Ключові слова: виділення кисню, побічний процес, гідроксид нікелю, Ni(OH)₂, циклічна вольтамперна крива

Предложена методика определения параметров выделения кислорода на оксиднонікеловом электроде. Предложенная методика применена для изучения процесса выделения кислорода на образцах гидроксида никеля, полученных разными способами и для различных фракций. Определены эффективные константы уравнения Тафеля. Показано, что параметры выделения кислорода зависят от метода получения гидроксида никеля (II) и его фракционного состава

Ключевые слова: выделение кислорода, побочный процесс, гидроксид никеля, Ni(OH)₂, циклическая вольтамперная кривая

UDC 54.057:544.653:621.13:661.13

DOI: 10.15587/1729-4061.2017.109770

COMPARISON OF OXYGEN EVOLUTION PARAMETERS ON DIFFERENT TYPES OF NICKEL HYDROXIDE

V. Kotok

PhD, Associate Professor*

Department of Processes, Apparatus and General Chemical Technology**

E-mail: valeriykotok@gmail.com

V. Kovalenko

PhD, Associate Professor*

Department of Analytical Chemistry and Food Additives and Cosmetics**

E-mail: vadimchem@gmail.com

V. Malyshev

Postgraduate student

Department of Technical Electrochemistry**

E-mail: valerii.v.malyshev@gmail.com

*Department of Technologies of

Inorganic Substances and Electrochemical Manufacturing Vyatka State University

Moskovskaya str., 36, Kirov, Russian Federation, 610000

**Ukrainian State University of Chemical Technology

Gagarina ave., 8, Dnipro, Ukraine, 49005

1. Introduction

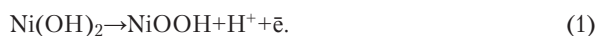
Ni(OH)₂ is used in batteries [1, 2] and asymmetric supercapacitors [3, 4] as an active material for positive elec-

trodes. This compound is also used in other fields: oxidation of organic compounds [5], sensors [6], electrochromic films [7, 8], fuel-cell electrode [9]. Interestingly, the mentioned applications are not the only ones, and lately the nickel oxide

films [10, 11] are viewed as components for dye-sensitized solar cells. The NiO for these cells is prepared via decomposition of nickel hydroxide, which is precipitated using various methods.

Because the number of directions, in which nickel oxide-hydroxide materials are used, is growing continuously, the relevance of studying the properties of this material remains high. The latter is supported not by a number of applied papers in various fields of nickel hydroxide applications [12, 13] but by theoretical papers as well [14, 15]. Theoretical papers regarding Ni(OH)₂ summarize the newest information about the material and recent progress on application and preparation [16, 17].

It is known that during charge (oxidation) of nickel hydroxide, a solid-state reaction (1) occurs at the electrode, and during discharge (reduction) the reaction (1) occurs in the reverse direction:



Along with oxidation, a side process of oxygen evolution occurs according to reaction (2):



This reaction plays a significant role in the effectiveness and charge (oxidation) rate of hydroxide. Reaction (2) is thermodynamically favored over reaction (1), so nickel oxidation and oxygen evolution occur simultaneously. Considering that hydroxide charging and oxygen evolution are competing processes, the parameters of nickel hydroxide would determine the effectiveness of the oxidation process. Therefore, the determination of the relation between oxygen evolution characteristics and type of used hydroxide is an important element for understanding and improving the effectiveness of processes that occur at nickel oxide electrodes.

2. Literature review and problem statement

As previously mentioned, the oxygen evolution during anodic polarization of the nickel oxide electrode is an undesirable process that lowers the effectiveness and increases charge duration of the chemical power source [18]. Another negative aspect of oxygen evolution is loss of electrical contact between active material and the current collector, because of intensive oxygen evolution, which leads to irreversible loss of electrode capacity [19]. Additionally, the decomposition of electrolyte and possible pressure buildup in sealed power sources can also be considered negative factors. These issues are solved by incorporation of valves into the frame of the power source or by employing specially designed counter-electrode, at which oxygen is reduced to water.

Oxygen evolution at the nickel oxide electrode is a complex reaction that consists of several stages. During these stages, various ions and particles are involved and formed: OH⁻, adsorbed OH and O⁻ [20]. It is also stated that two mechanisms of O₂ evolution exist, and the bend on Tafel curves corresponds to the change of oxygen evolution mechanism.

The paper [21] demonstrates that at high charge rates, the O₂ evolution is determined by the Ni³⁺/Ni²⁺ ratio. It has also been shown that introduction of Li⁺ changes the oxygen evolution mechanism on nickel oxide electrodes.

It is also interesting to note that the presence of dissolved oxygen in the electrolyte can add to the discharge capacity due to the reduction of O₂ to water [22].

In order to increase the polarization of oxygen evolution at the nickel oxide electrode, a number of researchers propose different approaches. In [23], it is proposed to coat nickel hydroxide with a layer of metallic cobalt in order to increase the polarization of oxygen evolution. It is stated that the use of such material leads to an increase of oxygen evolution polarization.

Other researchers [24] proposed a different approach, which lies in limiting the charge potential. It's been established that charging potential should be limited to 0.55 V (vs. Hg/HgO). Exceeding this limit leads to degradation in the electrode's capacity because of a large amount of evolved oxygen.

It should also be noted that there are numerous papers in which nickel oxide electrode is viewed for water decomposition [25, 26]. Thus, in the paper [27], it is stated that during oxygen evolution, the ageing of active material occurs, which leads to an increase of polarization of O₂ evolution. In addition, a special regime is proposed, in order to avoid electrode ageing. This regime allows maintaining low oxygen evolution overpotential resulting in lower water decomposition voltage.

In the paper [28], it is proposed to use mixed iron-nickel oxide (hydroxide), which allows conducting water decomposition at a lower voltage due to the lower polarization of oxygen evolution at such anode.

The conducted analysis allows stating that the problem of determining and comparing the oxygen evolution parameters for different applications is important and necessary. Such evaluation would allow determining the suitability of a synthesis method for specific applications.

3. The aim and objectives of the study

The aim of the work is to compare the parameters of oxygen evolution at nickel hydroxide powders that were synthesized using different methods and have different grain size. This would allow determining the influence of synthesis method on the oxygen evolution process, enabling to optimize synthesis methods for different applications.

To achieve the set aim, the following objectives were formulated:

- to choose the method conditions for determining the parameters of O₂ evolution;
- to study the morphology, composition and structure of two hydroxide types that were synthesized using different methods and have different grain size;
- to compare O₂ evolution parameters for different powders.

4. Materials and methods used in the study

Two types of nickel hydroxide powders were used. The first sample is commercially-available chemically precipitated nickel hydroxide powder of the Czech manufacturer "Bochemie" (denoted as Bochemie). The second sample was prepared using a slit-diaphragm electrolyzer (SDE) at a current density of 12 A/dm² (denoted as Ech12).

For SDE synthesis, NiSO_4 and NaOH were used as catholyte and anolyte. The synthesis procedure was carried out according to the literature [1, 29].

For the commercial sample, the powders with the grain size of 0–40 and 0–70 μm were used. The grain size of the electrochemical sample was 0–70 μm . The material's grain size was used in order to evaluate the influence of specific surface area on effective constants of the Tafel equation.

In order to determine the polarization of oxygen evolution, a potentiostatic method was proposed. It was assumed that upon setting a specific potential value in the region of nickel oxide charge, a rapid current increase would be observed at the initial time period t^* (Fig. 1). Then, the current would decrease to a certain value I_∞ after some time. The latter is related to the current redistribution into two processes: electrode charging to a certain amount of charge (that corresponds to this potential) and oxygen evolution. Theoretically, after the potential had been set, the current would be constant over an infinite period of time. However, it had been assumed that it is possible to experimentally find the moment at which the current value would be practically constant. That current value can be considered the current corresponding to oxygen evolution.

The Nernst equation was used to calculate oxygen evolution potential.

Before the experiment, the electrode was cycled at the following conditions: 0.2–0.7 V (NHE), 1 mV/s, 5 cycles. All experiments were conducted in the YSE-2 electrochemical cell (Fig.2) with 6M KOH as an electrolyte. The working electrode was made of nickel foil welded onto a 71 μm nickel mesh, on which the active mass was pasted. The active mass composition is listed in Table 1. Nickel mesh was used as counter-electrode. Ag/AgCl (KCl sat.) was used as reference electrode.

Table 1

Active mass composition for electrodes in experiments

No.	Component	% wt.
1	$\text{Ni}(\text{OH})_2$	74
2	Graphite (GAK-3)	16
3	PTFE (F-4D)	10

For uniform distribution of current density, the working electrode was placed into a dielectric cassette. The electrode area was 3.6 cm^2 .

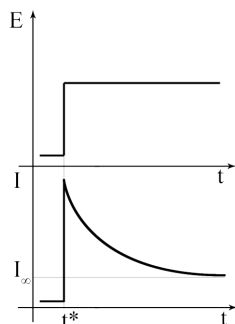


Fig. 1. Dependency of current (I) versus time (t) at the set potential in the charging region of nickel oxide electrode

After cycling, the potential steps of 0.60, 0.62, 0.64, 0.66, and 0.68 V (NHE) were used in all experiments. Two electrodes were made for each powder type. After initial cycling,

both electrodes were kept at different potentials and changes in current with time were recorded. One electrode was cycled from more negative to more positive potentials (forward scan) and the other was cycled backwards (backward scan). This was done in order to determine the difference between results acquired at decreasing and increasing potential.

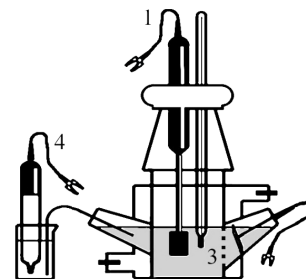


Fig. 2. Cell used for potentiostatic cycling and determining oxygen evolution parameters: 1 – working electrode; 2 – counter-electrode; 3 – electrolyte; 4 – reference electrode

Sample morphology was determined by means of Scanning Electron Microscopy (SEM). SEM images were recorded on JEOL JSM-6510 LV (Japan).

Sample composition was evaluated by means of Energy Dispersive X-ray analysis (EDX), using JEOL JEM-2100 (Japan).

IR spectra were recorded on Bruker Tensor 27 (USA).

In order to determine the structure of prepared materials, the XRD patterns of powders were recorded using DRON-3 diffractometer (Russian Federation), Co-K α monochromatic radiation.

5. Morphology, structure and composition analysis of $\text{Ni}(\text{OH})_2$ samples used in the experiment

In order to understand the difference between the physico-chemical properties of the powders chosen for the experiment, analyses that allow determining the morphology, crystal structure and composition of the samples were conducted.

The results of SEM have revealed a significant difference in the morphology of the powders. The sample Bochemie demonstrates a shard-like morphology, no distinct structures can be outlined – Fig. 3, *a, b*. For the electrochemically synthesized sample, a mixed morphology had been discovered. The sample consists of two particle types: shard-like forms and plates with unordered orientation – Fig. 3, *c, d*.

The XRD patterns (Fig. 4) have confirmed significant structural differences of both samples. In comparison to the electrochemically prepared samples (Ech12), the sample Bochemie shows a high degree of structural order, which is indicated by high and well-defined peaks. It should also be noted that the sample Bochemie corresponds to the β -form, because the first peak is situated at about 23°.

The sample Ech12 demonstrates a low degree of order and low crystallinity, which is indicated by the absence of defined peaks on the XRD pattern. It should also be noted that the first peak of the α -form is situated at 12–13°. Because the XRD pattern shows some signal increase in the region from 10 to 24°, it was concluded that the sample is composed of layers of α and β -forms.

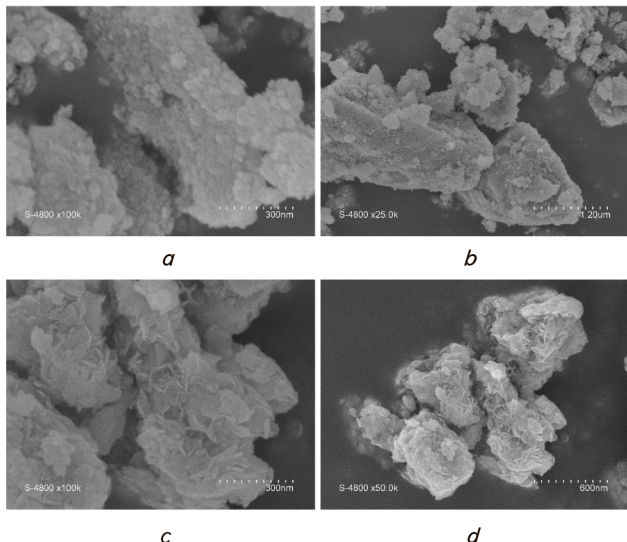


Fig. 3. SEM images of Ni(OH)₂ powders used in the study: a, b – Boehemie; c, d – Ech12

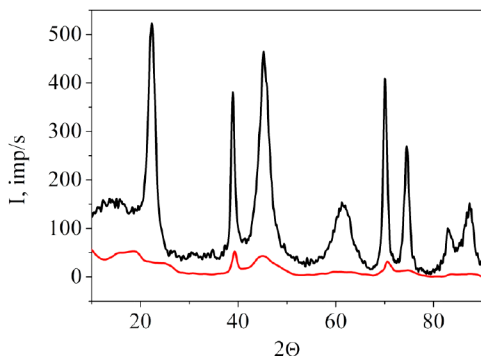


Fig. 4. XRD patterns of Ni(OH)₂ powders used in the study: Boehemie (black); Ech12 (red)

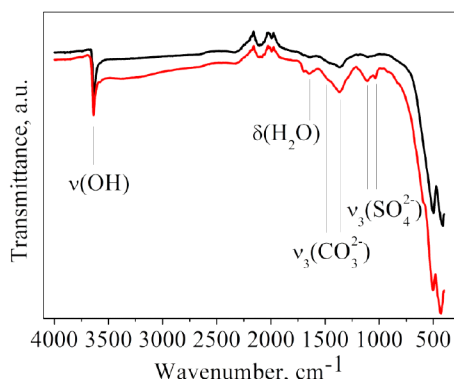


Fig. 5 IR-spectra of Ni(OH)₂ powders used in the study: Boehemie (black); Ech12 (red)

The analysis of IR spectra has also revealed differences between the samples. Thus, the pattern of the electrochemically precipitated sample (Fig. 5, red line) shows more pronounced absorption bands of bound water, carbonate and sulfate ions, indicating their higher content in Ech12 [30–33]. This is also supported by the results of EDX analysis – Table 2, 3.

By analyzing the data from Tables 3, 4, it can be seen that in comparison to the sample Boehemie, the Ech12 contains significantly more sulfur and about twice as much carbon.

Table 2

Elemental composition of Boehemie Ni(OH)₂ sample (wt. %)

Point	C	O	Ni
1	4.19	45.98	49.83
2	3.99	47.2	48.81

Table 3

Elemental composition of Ech12 Ni(OH)₂ sample (wt. %)

Point	C	O	S	Co	Ni
1	8.33	51.41	1.45	0.47	38.34
2	7.66	47.84	1.5		43

5. 1. Results of determining oxygen evolution parameters

As a result of cycling, six cyclic voltamperograms were recorded, three of which are presented in Fig. 6–8. The analysis of cyclic voltamperograms allows concluding that oxygen evolution occurs at the potential values about 0.6 V and above. It can also be added that the charge peak potential for the industrial sample is at more positive values (≈0.56 V) than that of electrochemically prepared samples (≈0.53 V). Also, the curve region that corresponds to oxygen evolution is more slanted for the sample Ech12.

The next step was to obtain a series of curves, according to Fig. 1. The initial tests have revealed that after setting the potential value, the current indeed starts to drop after some period of time, however, at potentials above 0.62 V, the different behavior is observed: the current value decreased initially, but after some time it started to increase. This interesting behavior is likely related to the following: when the electrode is kept at high potentials over an extended period of time, α-NiOOH starts to transform into γ-NiOOH, according to the Bode diagram (Fig. 5) [34]. The lattice parameter C of γ-NiOOH is approximately 4 times higher than that of α-NiOOH. During the formation of γ-NiOOH, the crystals change their volume in different directions of the polycrystalline particle, causing its breakdown, increase and exposure of the active material surface. The previously hidden surface contains less charge, which results in increased current because of imitate charging of the newly exposed surface. The described process could be repeatable.

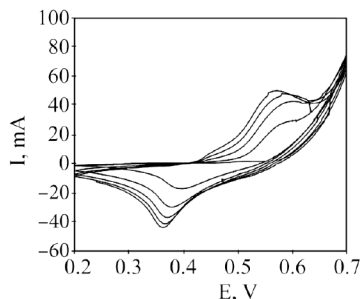


Fig. 6. Cyclic voltamperogram of the sample Boehemie (grain size 0–70 μm)

In order to minimize the experimental time, it was proposed to stop the experiment according to the condition, which is described by the inequality (3):

$$|i_{15}^n - i_{15}^p| \leq (i_{60} \cdot 0.05) \cdot 1/4, \tag{3}$$

where i_{60} – the current density after an hour has passed after setting the potential value; i_{15}^n and i_{15}^{p-1} – current densities after each quarter of an hour after an hour of the experiment had passed (n – next p – previous).

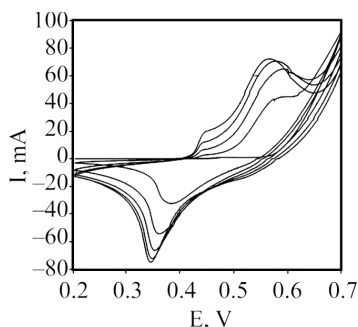


Fig. 7. Cyclic voltamperogram of the sample Bochemie (grain size 0–40 μm)

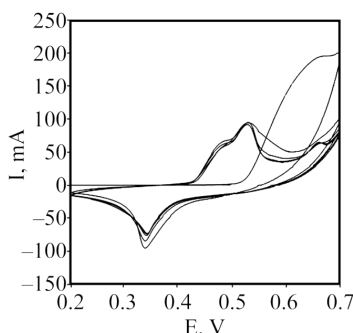


Fig. 8. Cyclic voltamperogram of the sample Ech12 (grain size 0–40 μm)

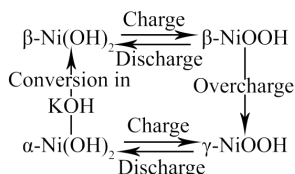


Fig. 9. Bode diagram

Thus, if the current density decrease was less or equal to 5 % of the current density recorded after the initial hour, the experiment was stopped, and the established value was considered to be the current density of oxygen evolution. In these cases, the condition was not taken into account, and the current density at which bend occurs was taken as the current density of oxygen evolution.

It should be noted that for all calculations, the working area of the electrode was used, and not the actual surface of the powders. Additionally, the electrodes were composed of a mixture of nickel hydroxide, graphite and PTFE emulsion, which only allows finding some effective values that can only be compared to each other.

It should also be noted that the graphs plotted in the coordinates polarization – current density logarithm were almost straight lines when converted to Tafel coordinates. This proves the validity of the chosen experiment methodology.

The obtained data were used to calculate effective constants for the Tafel equation, which are presented in Fig. 10, 11.

It can be seen that during forward and backward scans, the effective constants a_{eff} and b_{eff} do not differ significantly,

which also indicates the correctness of the chosen approach. It can also be said that the method and the grain size do affect the resulting values of effective constants. Obviously, the slope and the positions of both curves would differ significantly with the charge current density. Therefore, it was decided to plot the graphs in Tafel coordinates using averaged values of a_{eff} and b_{eff} for forward and backward scans. The results are presented in Fig 12.

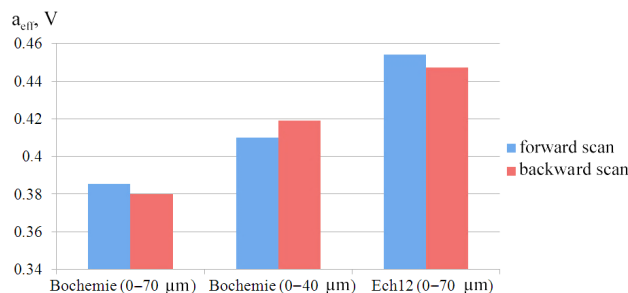


Fig. 10. a_{eff} histograms for different nickel hydroxides and different grain sizes

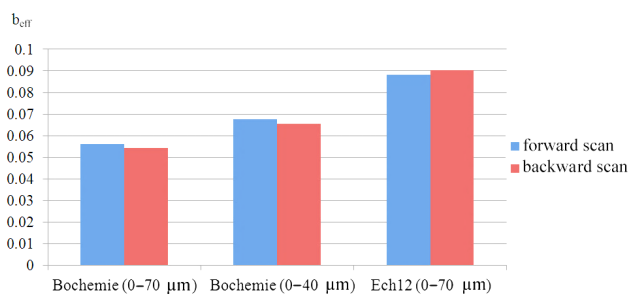


Fig. 11. b_{eff} histograms for different nickel hydroxides and different grain sizes

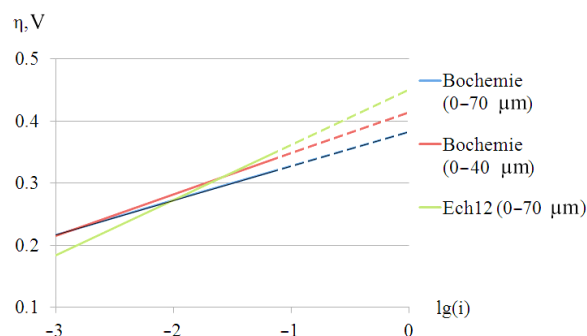


Fig. 12. Graphs plotted using averaged effective constants a_{eff} and b_{eff} for different samples

This result is interesting because this graph allows determining the changes in polarization of oxygen evolution at different charge current densities. At low current densities of 0.001 A/cm^2 ($\lg(i)=-3$), the polarization is lower for both grain sizes of industrial hydroxide. When the current density was increased to 0.01 A/cm^2 ($\lg(i)=-2$), the polarizations of the powders Bochemie (0–70 μm grain size) and Ech12 (0–70 μm grain size) are matched, while the powder Bochemie (0–40 μm grain size) has a higher polarization. At the current density of about 0.025 A/cm^2 ($\lg(i)=-1.6$), the polarizations of oxygen evolution for the samples Bochemie (0–40 μm grain size) and Ech12 (0–70 μm grain size) are matched, while decreasing for the sample Bochemie (0–70 μm grain size). At current densities higher than

0.025 A/cm², the highest polarization of oxygen evolution is observed for the sample Ech12, followed by the samples Bochemie (0–40 μm grain size), and Bochemie (0–70 μm grain size). The preliminary conclusion is that at low current densities, the oxygen evolution is higher for industrial samples, while at high – for the electrochemically prepared sample.

6. Discussion of the results of study on polarization of oxygen evolution on nickel hydroxides

When determining the physico-chemical characteristics of nickel hydroxide powders, it had been demonstrated that electrochemically prepared nickel hydroxide (Ech12) and industrial Bochemie differ significantly in morphology, composition and structure.

It had been shown that the surface of the sample Ech12 contains shard-like and plate-like particles, while that of industrial samples is only composed of shard-like particles. The samples structure was also significantly different. The industrial Ni(OH)₂ had a high degree of crystallinity and contained the β phase. The electrochemical samples had low crystallinity and a large number of defects and contained α and β phases. Two different analyses have revealed the presence of large amounts of bound water, carbonate and sulfate ions in electrochemically prepared Ni(OH)₂. Thus, the polarizations of oxygen evolution on two types of nickel hydroxides that have significantly different physico-chemical characteristics have been studied.

Preliminary experiments have resulted in a methodology that allowed obtaining effective constants of the Tafel equation for the selected powders. The obtained polarization-current density logarithm graphs were almost perfectly straight for all the samples. It also had been revealed that the values acquired from forward and backward scans don't have a significant impact on the obtained constants, and the difference between the two was no more than 10 % in relation to the lowest value. Therefore, the authors have concluded that the methodology can be used to evaluate the oxygen evolution process.

The oxygen evolution parameters (a_{eff} and b_{eff}) for all nickel hydroxide samples relative to oxygen evolution parameters have revealed that the O₂ evolution process during the charge process depends on the type of Ni(OH)₂, which is determined by synthesis method and conditions, and on the grain size, which determines the specific surface area.

It should be said that industrial nickel hydroxide powders with different grains sizes have demonstrated high polarization at low current densities. Higher current density led to a greater increase of polarization for the sample with smaller grain size (0–40 μm) than for the sample with larger

grain size (0–70 μm). At high current densities, the polarization was higher for the electrochemically prepared nickel hydroxide sample. Nevertheless, the presence and intensity of oxygen evolution are not the only factors that affect the charging process. The process is also affected by the position of the charge peak and parameters of the hydroxide – proton diffusion coefficient, specific surface area, which depend on structure and composition. Therefore, the further study on the efficiency of the charging process should be combined with an investigation of the oxygen evolution process and charge-discharge characteristics.

7. Conclusions

1. A method for determining the polarization of oxygen evolution at nickel oxide electrodes has been developed and its parameters have been established. The presented methodology has a good reproducibility and can be used for evaluative comparison of O₂ evolution at different types of Ni(OH)₂.

2. It was demonstrated that the samples used in experiments have different morphology, structure and composition. The industrial β-Ni(OH)₂ sample has a shard-like structure, high degree of crystallinity and doesn't contain intercalation anions. The electrochemically prepared sample has a low degree of crystallinity and has a structure that is composed of α and β-forms that contain carbonate and sulfate ions.

3. Oxygen evolution parameters for the hydroxides that were synthesized using different methods and had different grain size have been determined. It had been demonstrated that in addition to morphology, the structure and grain size of the powder significantly affect the oxygen evolution parameters. For the sample that was electrochemically prepared, the averaged values of a_{eff} and b_{eff} are 0.451, and 0.089, respectively. In turn, the average values of a_{eff} and b_{eff} for industrial samples are 0.383, 0.055 (0–70 μm) and 0.414, 0.067 (0–40 μm), respectively.

Acknowledgments

The authors wish to express their gratitude to the staff of the Montpellier University (France) for the provided assistance in the study, and personally to: professors F. Henn, J.-L. Bantignies, A. Mehdi, and Ph.D. S. Deabate. The authors also wish to express their gratitude to Campus France, French Institute in Ukraine and French Embassy in Ukraine for providing the possibility to conduct the research in France.

References

1. Kovalenko, V. Definition of factors influencing on Ni(OH)₂ electrochemical characteristics for supercapacitors [Text] / V. Kovalenko, V. Kotok, O. Bolotin // Eastern-European Journal of Enterprise Technologies. – 2016. – Vol. 5, Issue 6 (83). – P. 17–22. doi: 10.15587/1729-4061.2016.79406
2. Kovalenko, V. L. Nickel hydroxide obtained by high-temperature two-step synthesis as an effective material for supercapacitor applications [Text] / V. L. Kovalenko, V. A. Kotok, A. A. Sykchin, I. A. Mudryi, B. A. Ananchenko, A. A. Burkov et. al. // Journal of Solid State Electrochemistry. – 2016. – Vol. 21, Issue 3. – P. 683–691. doi: 10.1007/s10008-016-3405-2
3. Kovalenko, V. Study of the influence of the template concentration under homogeneous precepitation on the properties of Ni(OH)₂ for supercapacitors [Text] / V. Kovalenko, V. Kotok // Eastern-European Journal of Enterprise Technologies. – 2017. – Vol. 4, Issue 6 (88). – P. 17–22. doi: 10.15587/1729-4061.2017.106813

4. Kotok, V. The properties investigation of the faradaic supercapacitor electrode formed on foamed nickel substrate with poly-vinyl alcohol using [Text] / V. Kotok, V. Kovalenko // Eastern-European Journal of Enterprise Technologies. – 2017. – Vol. 4, Issue 12 (88). – P. 31–37. doi: 10.15587/1729-4061.2017.108839
5. Solovov, V. Influence of temperature on the characteristics of Ni(II), Ti(IV) layered double hydroxides synthesised by different methods [Text] / V. Solovov, V. Kovalenko, N. Nikolenko, V. Kotok, E. Vlasova // Eastern-European Journal of Enterprise Technologies. – 2017. – Vol. 1, Issue 6 (85). – P. 16–22. doi: 10.15587/1729-4061.2017.90873
6. Miao, F. Ordered-standing nickel hydroxide microchannel arrays: Synthesis and application for highly sensitive non-enzymatic glucose sensors [Text] / F. Miao, B. Tao, P. K. Chu // Microelectronic Engineering. – 2015. – P. 11–15. doi: 10.1016/j.mee.2014.11.005
7. Kotok, V. A. Advanced electrochromic Ni(OH)₂/PVA films formed by electrochemical template synthesis [Text] / V. A. Kotok, V. L. Kovalenko, P. V. Kovalenko, V. A. Solovov, S. Deabate, A. Mehdi et. al. // ARPN Journal of Engineering and Applied Sciences. – 2017. – Vol. 12, Issue 13. – P. 3962–3977.
8. Kotok, V. The electrochemical cathodic template synthesis of nickel hydroxide thin films for electrochromic devices: role of temperature [Text] / V. Kotok, V. Kovalenko // Eastern-European Journal of Enterprise Technologies. – 2017. – Vol. 2, Issue 11 (86). – P. 28–34. doi: 10.15587/1729-4061.2017.97371
9. Huang, W. Highly active and durable methanol oxidation electrocatalyst based on the synergy of platinum–nickel hydroxide–graphene [Text] / W. Huang, H. Wang, J. Zhou, J. Wang, P. N. Duchesne, D. Muir et. al. // Nature Communications. – 2015. – Vol. 6. – P. 10035. doi: 10.1038/ncomms10035
10. Ranganathan, P. Enhanced photovoltaic performance of dye-sensitized solar cells based on nickel oxide supported on nitrogen-doped graphene nanocomposite as a photoanode [Text] / P. Ranganathan, R. Sasikumar, S.-M. Chen, S.-P. Rwei, P. Sireesha // Journal of Colloid and Interface Science. – 2017. – Vol. 504. – P. 570–578. doi: 10.1016/j.jcis.2017.06.012
11. Huo, J. Fabrication a thin nickel oxide layer on photoanodes for control of charge recombination in dye-sensitized solar cells [Text] / J. Huo, Y. Tu, M. Zheng, J. Wu // Journal of Solid State Electrochemistry. – 2017. – Vol. 21, Issue 6. – P. 1523–1531. doi: 10.1007/s10008-017-3515-5
12. Malara, F. A Flexible Electrode Based on Al-Doped Nickel Hydroxide Wrapped around a Carbon Nanotube Forest for Efficient Oxygen Evolution [Text] / F. Malara, S. Carallo, E. Rotunno, L. Lazzarini, E. Piperopoulos, C. Milone, A. Naldoni // ACS Catalysis. – 2017. – Vol. 7, Issue 7. – P. 4786–4795. doi: 10.1021/acscatal.7b01188
13. Qiu, C. Corrosion resistance and micro-tribological properties of nickel hydroxide-graphene oxide composite coating [Text] / C. Qiu, D. Liu, K. Jin, L. Fang, T. Sha // Diamond and Related Materials. – 2017. – Vol. 76. – P. 150–156. doi: 10.1016/j.diamond.2017.04.015
14. Hall, D. S. Nickel hydroxides and related materials: a review of their structures, synthesis and properties [Text] / D. S. Hall, D. J. Lockwood, C. Bock, B. R. MacDougall // Proceedings of the Royal Society A: Mathematical, Physical and Engineering Sciences. – 2014. – Vol. 471, Issue 2174. – P. 20140792–20140792. doi: 10.1098/rspa.2014.0792
15. Vidotti, M. Eletrodos modificados por hidróxido de níquel: um estudo de revisão sobre suas propriedades estruturais e eletroquímicas visando suas aplicações em eletrocatalise, eletrocromismo e baterias secundárias [Text] / M. Vidotti, R. Torresi, S. I. C. de Torresi // Química Nova. – 2010. – Vol. 33, Issue 10. – P. 2176–2183. doi: 10.1590/s0100-40422010001000030
16. Yan-wei, L. Progress in research on amorphous nickel hydroxide electrode materials [Text] / L. Yan-wei, L. Chang-jiu, Y. Jinhuan // Xiandai Huagong/Modern Chemical Industry. – 2010. – Vol. 30, Issue 2. – P. 25–27.
17. Feng, L. Recent progress in nickel based materials for high performance pseudocapacitor electrodes [Text] / L. Feng, Y. Zhu, H. Ding, C. Ni // Journal of Power Sources. – 2014. – Vol. 267. – P. 430–444. doi: 10.1016/j.jpowsour.2014.05.092
18. Snook, G. A. Detection of Oxygen Evolution from Nickel Hydroxide Electrodes Using Scanning Electrochemical Microscopy [Text] / G. A. Snook, N. W. Duffy, A. G. Pandolfo // Journal of The Electrochemical Society. – 2008. – Vol. 155, Issue 3. – P. A262. doi: 10.1149/1.2830837
19. Kotok, V. Optimization of nickel hydroxide electrode of the hybrid supercapacitor [Text] / V. Kotok, V. Kovalenko // Eastern-European Journal of Enterprise Technologies. – 2017. – Vol. 1, Issue 6 (85). – P. 4–9. doi: 10.15587/1729-4061.2017.90810
20. Bronoel, G. Mechanism of oxygen evolution in basic medium at a nickel electrode [Text] / G. Bronoel, J. Reby // Electrochimica Acta. – 1980. – Vol. 25, Issue 7. – P. 973–976. doi: 10.1016/0013-4686(80)87102-7
21. Nadesan, J. C. B. Oxygen Evolution on Nickel Oxide Electrodes [Text] / J. C. B. Nadesan // Journal of The Electrochemical Society. – 1985. – Vol. 132, Issue 12. – P. 2957. doi: 10.1149/1.2113700
22. Motupally, S. The Role of Oxygen at the Second Discharge Plateau of Nickel Hydroxide [Text] / S. Motupally // Journal of The Electrochemical Society. – 1998. – Vol. 145, Issue 1. – P. 34. doi: 10.1149/1.1838206
23. Wang, X. Oxygen catalytic evolution reaction on nickel hydroxide electrode modified by electroless cobalt coating [Text] / X. Wang // International Journal of Hydrogen Energy. – 2004. – Vol. 29, Issue 9. – P. 967–972. doi: 10.1016/j.ijhydene.2003.05.001

24. Snook, G. A. Evaluation of the effects of oxygen evolution on the capacity and cycle life of nickel hydroxide electrode materials [Text] / G. A. Snook, N. W. Duffy, A. G. Pandolfo // *Journal of Power Sources*. – 2007. – Vol. 168, Issue 2. – P. 513–521. doi: 10.1016/j.jpowsour.2007.02.060
25. Lyons, M. E. G. Redox Switching and Oxygen Evolution at Hydrous Oxyhydroxide Modified Nickel Electrodes in Aqueous Alkaline Solution: Effect of Hydrous Oxide Thickness and Base Concentration [Text] / M. E. G. Lyons, L. Russell, M. O'Brien, R. L. Doyle, I. Godwin, M. P. Brandon // *Int. J. Electrochem. Sci.* – 2012. – Vol. 7. – P. 2710–2763.
26. Lyons, M. E. G. Hydrous Nickel Oxide: Redox Switching and the Oxygen Evolution Reaction in Aqueous Alkaline Solution [Text] / M. E. G. Lyons, R. L. Doyle, I. Godwin, M. O'Brien, L. Russell // *Journal of the Electrochemical Society*. – 2012. – Vol. 159, Issue 12. – P. H932–H944. doi: 10.1149/2.078212jes
27. Mellso, S. R. Electrocatalytic oxygen evolution on nickel oxy-hydroxide anodes: Improvement through rejuvenation [Text] / S. R. Mellso, A. Gardiner, A. T. Marshall // *Electrochimica Acta*. – 2015. – Vol. 180. – P. 501–506. doi: 10.1016/j.electacta.2015.08.061
28. Bau, J. A. Oxygen Evolution Catalyzed by Nickel–Iron Oxide Nanocrystals with a Nonequilibrium Phase [Text] / J. A. Bau, E. J. Luber, J. M. Buriak // *ACS Applied Materials & Interfaces*. – 2015. – Vol. 7, Issue 35. – P. 19755–19763. doi: 10.1021/acsami.5b05594
29. Kovalenko, V. Obtaining of Ni–Al layered double hydroxide by slit diaphragm electrolyzer [Text] / V. Kovalenko, V. Kotok // *Eastern-European Journal of Enterprise Technologies*. – 2017. – Vol. 2, Issue 6 (86). – P. 11–17. doi: 10.15587/1729-4061.2017.95699
30. Kotok, V. Electrochromism of Ni(OH)₂ films obtained by cathode template method with addition of Al, Zn, Co ions [Text] / V. Kotok, V. Kovalenko // *Eastern-European Journal of Enterprise Technologies*. – 2017. – Vol. 3, Issue 12 (87). – P. 38–43. doi: 10.15587/1729-4061.2017.103010
31. Oliva, P. Review of the structure and the electrochemistry of nickel hydroxides and oxy-hydroxides [Text] / P. Oliva, J. Leonardi, J. F. Laurent, C. Delmas, J. J. Braconnier, M. Figlarz et. al. // *Journal of Power Sources*. – 1982. – Vol. 8, Issue 2. – P. 229–255. doi: 10.1016/0378-7753(82)80057-8
32. Genin, P. Preparation and characterization of α -type nickel hydroxides obtained by chemical precipitation: study of the anionic species [Text] / P. Genin, A. Delahaye-Vidal, F. Portemer, K. Tekaia-Elhsissen, M. Figlarz // *Eur. J. Solid State Inorg. Chem.* – 1991. – Vol. 28. – P. 505.
33. Faure, C. Characterization of a turbostratic α -nickel hydroxide quantitatively obtained from an NiSO₄ solution [Text] / C. Faure, C. Delmas, M. Fouassier // *Journal of Power Sources*. – 1991. – Vol. 35, Issue 3. – P. 279–290. doi: 10.1016/0378-7753(91)80112-b
34. Delahaye-Vidal, A. Structural and textural investigations of the nickel hydroxide electrode [Text] / A. Delahaye-Vidal // *Solid State Ionics*. – 1996. – Vol. 84, Issue 3-4. – P. 239–248. doi: 10.1016/0167-2738(96)00030-6
35. Srinivasan, V. Mathematical models of the nickel hydroxide active material [Text] / V. Srinivasan, J. W. Weidner, R. E. White // *Journal of Solid State Electrochemistry*. – 2000. – Vol. 4, Issue 7. – P. 367–382. doi: 10.1007/s100080000107